

Sussex Research

Fovea-like photoreceptor specializations underlie single UV cone driven prey-capture behavior in zebrafish

Takeshi Yoshimatsu, Cornelius Schröder, Noora Nevala, Philipp Berens, Thomas Baden

Publication date

22-07-2020

Licence

This work is made available under the CC BY 4.0 licence and should only be used in accordance with that licence. For more information on the specific terms, consult the repository record for this item.

Document Version

Published version

Citation for this work (American Psychological Association 7th edition)

Yoshimatsu, T., Schröder, C., Nevala, N., Berens, P., & Baden, T. (2020). *Fovea-like photoreceptor specializations underlie single UV cone driven prey-capture behavior in zebrafish* (Version 2). University of Sussex. https://hdl.handle.net/10779/uos.23308316.v2

Published in

Neuron

Link to external publisher version

https://doi.org/10.1016/j.neuron.2020.04.021

Copyright and reuse:

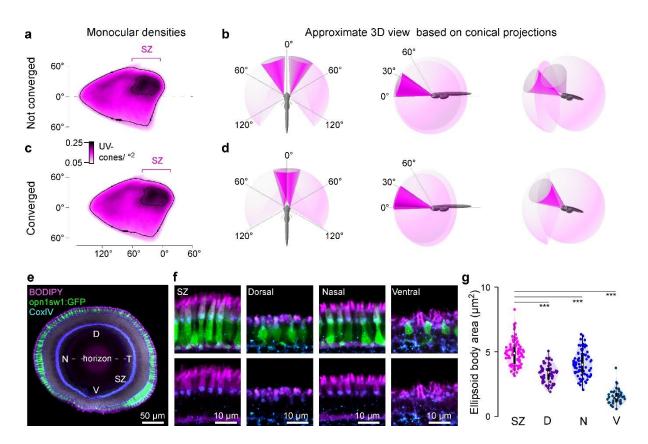
This work was downloaded from Sussex Research Open (SRO). This document is made available in line with publisher policy and may differ from the published version. Please cite the published version where possible. Copyright and all moral rights to the version of the paper presented here belong to the individual author(s) and/or other copyright owners unless otherwise stated. For more information on this work, SRO or to report an issue, you can contact the repository administrators at sro@sussex.ac.uk. Discover more of the University's research at https://sussex.figshare.com/

SUPPLEMENTARY MATERIALS

Fovea-like photoreceptor specialisations underlie single UV-cone driven prey

capture behaviour in zebrafish

Yoshimatsu et al.



SUPPLEMENTARY FIGURES AND LEGENDS

Figure S1, related to Figure 2. Structural specialisations of UV-cones for prey capture. *a*, Monocular UV-cone density projection into visual space when eyes are not converged. *b*, Schematics of approximate visual space surveyed by the two SZs (dark pink) and full field of view (light pink) when viewed from top (left), side (middle) and front/bottom (right). *c,d*, As (a,b), but when the eyes are converged. *e.* UV-cones (Tg(opn1sw1:GFP)) with BODIPY and mitochondria (CoxIV) counterstaining in a whole eye sagittal view. N, nasal; D, dorsal; T, temporal; SZ, strike zone; V, ventral. *f.* High magnification images of the same eye. *g*, Quantification of differences in ellipsoid body area between zones. Mann-Whitney U-test, ***: p<0.0001.

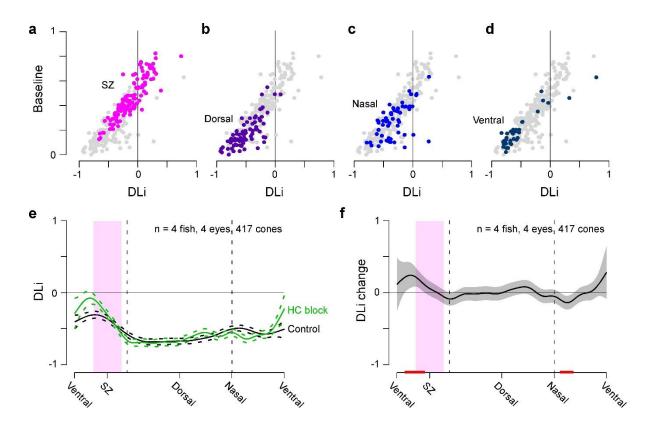


Figure S2, related to Figure 6. Baseline relation to DLi and horizontal cell block. a-d, Scatter plots of calcium baseline versus dark-light index (DLi) across zones, with full dataset (grey) superimposed by the individual zones as indicated. **e**, Mean and 95% confidence intervals of DLi before (black) and after (green) blockage of horizontal cell feedback by CNQX application. **f**, Change in DLi from (e), with red lines indicating significant change from 0.

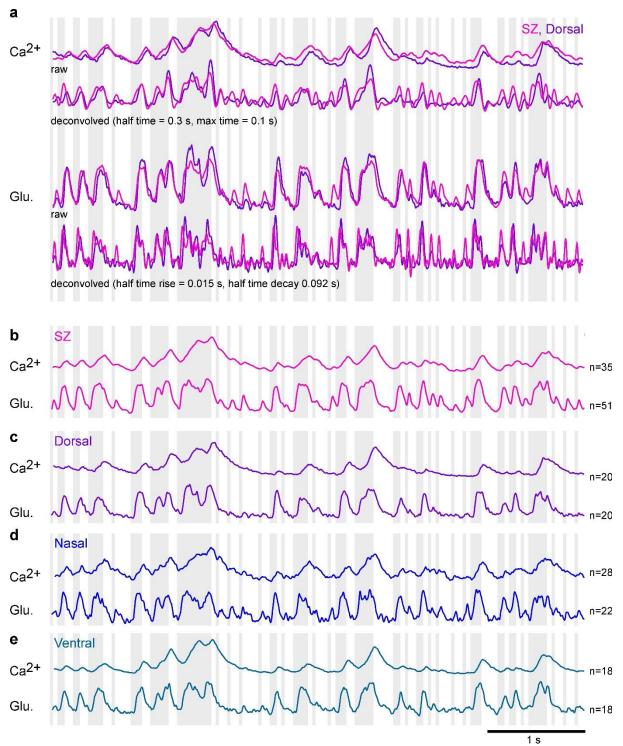


Figure S3, related to Figure 8. Comparison of glutamate and calcium responses across retinal regions. a. raw and deconvolved (Wiener deconvolution with calculated SNR using all recordings per zone (Ca^{2+} , T = 0.3 s) and SFiGluSnFR (glu., T = 0.092 s) responses from Fig. 8a to account for the kinetic differences between the sensors. The deconvolution does not strongly affect the differences between Dorsal and SZ UV-cones. **b-e.** Mean calcium and glutamate responses of UV-cones in the individual zones to the tetrachromatic noise stimulus. Background shading indicates UV-light and dark stimulus periods.

SUPPLEMENTARY VIDEOS

Supplementary Video S1, related to Figure 1. Detecting paramecia in UV and "yellow" wavebands. Video of paramecia in naturalistic tank as viewed in a "yellow" channel that is approximately aligned with zebrafish M- and L-cones (left), and the same scene subsequently filmed in a zebrafish-approximate UV channel (right). The yellow channel provides spatial detail of the background and underside of the water, which masks paramecia swimming in the foreground. In contrast, the UV channel does not resolve the background clutter but instead brings out paramecia illuminated by the sun as bright dots in the upper water column. Videos recorded at 10 Hz and played back in real time (Methods).

Supplementary Video S2 related to Figure 1. Example prey capture bout under UV. Top-view of 7 *dpf* zebrafish larva mounted in agarose with eyes and tail free to move. Free-swimming paramecia appear as dark moving "dots". Note prey-capture bout at t = 5 s.

Supplementary Video S3, related to Figure 3. Imaging UV-cone synaptic calcium in vivo. Calcium responses to bright- and dark-flashes in UV-cones from SZ (upper) and dorsal (D, bottom) as in Fig. 3b. The video is an average of 5 repeats of single trial raw movies that were cropped and aligned. The magenta bar indicates the timing of bright and dark flashes. Supplementary Video S4, related to Figure 5. A model of visual detectability of bright and dark moving objects. Left, modelled UV-cone detector array (top) and bipolar cells (bottom) responding to a bright 2° target moving in a pseudorandom path at 100°/s. The target is meant to mimic a paramecium. Right, as left, with target size increased to 5° and contrast inverted to dark. The target is meant to mimic a distant or small predator. In each case, the colour-scaling indicates relative activation of cones or bipolar cells scaled to the array's maximum. Note that the small light target is only readily detectable in the strike zone (top left in each array), while the predator is always detectable. Played back at real-time.

Supplementary Video S5, related to Figure 6. Whole-eye imaging of light-driven

UV-cone calcium levels. UV-cone calcium responses to bright- and dark-flashes as in Fig. 6. The video is an average of 7 repeats of single trial raw movies that were cropped and aligned. The bars on the right indicate the timing of bright and dark flashes and the RGB background, which are all superimposed on a constant UV-background (not indicated).

Supplementary Video S6, related to Figure 8. Imaging glutamate release from cones in vivo. Video of mean glutamate responses over n = 7 repetitions of the tetrachromatic binary noise stimulus as in Fig. 8. Green is SFiGluSnFR in HC and red is mCherry expression in UV-cones. The bars on the right indicate the timing of flashes of each LED.

Supplementary Video S7, related to Figure 8. Glutamate release differences between SZ and dorsal. Video of mean glutamate responses over n = 4 repetitions of the tetrachromatic binary noise stimulus as in Fig. 8. Green is SFiGluSnFR in HC and red is mCherry expression in UV-cones. Circles indicate UV-cone terminals shown in the bottom as high-magnification. The bars on the right indicate the timing of flashes of each LED.

SUPPLEMENTARY TABLES

Supplementary Table S1, related to Fig. 4b.

ANOVA test summary

ANOVA - Tau

Cases	Sum of Squares	df	Mean Square	F	р
Area	809303.707	3.000	269767.902	16.104	< .001
Residual	1.390e +6	83.000	16751.649		

Note. Type III Sum of Squares

Post Hoc Comparisons - Area

		Mean Difference	SE	t	p tukey
D	N	-53.251	38.166	-1.395	0.506
2	S	-232.995	36.138	-6.447	< .001
	V	-149.494	46.090	-3.244	0.009
Ν	S	-179.743	36.138	-4.974	< .001
	V	-96.243	46.090	-2.088	0.165
S	V	83.501	44.425	1.880	0.245

Supplementary Table S2, related to Fig. 4d.

ANOVA test summary

ANOVA - Tau

Cases	Sum of Squares	df	Mean Square	F	р
Area	309988.967	3.000	103329.656	5.220	0.002
Residual	1.504e +6	76.000	19794.247		

Note. Type III Sum of Squares

Post Hoc Comparisons - Area

		Mean Difference	SE	t	p _{tukey}
D	N	68.396	43.204	1.583	0.394
	S	98.500	40.206	2.450	0.076
	V	-79.960	49.742	-1.607	0.381
Ν	S	30.104	42.820	0.703	0.896
	V	-148.357	51.878	-2.860	0.027
S	V	-178.461	49.409	-3.612	0.003

Supplementary Table S3, related to Fig. 4f.

ANOVA test summary

ANOVA - Tau

Cases	Sum of Squares	df	Mean Square	F	р
Area	189940.750	3.000	63313.583	3.340	0.020
Condition	366672.408	1.000	366672.408	19.345	< .001
Area * Condition	495659.877	3.000	165219.959	8.717	< .001
Residual	5.364e +6	283.000	18954.580		

Note. Type III Sum of Squares

Post Hoc Comparisons - Area * Condition

		Mean Difference	SE	t	p tukey
D,CNQX	N,CNQX	-11.932	31.692	-0.376	1.000
	S,CNQX	67.183	31.048	2.164	0.377
	V,CNQX	-79.515	39.874	-1.994	0.488
	D,Normal	-3.256	35.298	-0.092	1.000
	N,Normal	-97.079	31.692	-3.063	0.049
	S,Normal	-138.231	31.048	-4.452	< .001
	V,Normal	-94.391	41.320	-2.284	0.306
N,CNQX	S,CNQX	79.115	27.995	2.826	0.093
	V,CNQX	-67.583	37.546	-1.800	0.621
	D,Normal	8.675	32.644	0.266	1.000
	N,Normal	-85.147	28.707	-2.966	0.064
	S,Normal	-126.299	27.995	-4.511	< .001
	V,Normal	-82.459	39.077	-2.110	0.411
S,CNQX	V,CNQX	-146.698	37.004	-3.964	0.002
	D,Normal	-70.439	32.020	-2.200	0.355
	N,Normal	-164.262	27.995	-5.868	< .001
	S,Normal	-205.414	27.264	-7.534	< .001
	V,Normal	-161.574	38.557	-4.191	< .001
V,CNQX	D,Normal	76.259	40.635	1.877	0.568
	N,Normal	-17.564	37.546	-0.468	1.000
	S,Normal	-58.716	37.004	-1.587	0.758
	V,Normal	-14.876	45.963	-0.324	1.000
D,Normal	N,Normal	-93.823	32.644	-2.874	0.082
	S,Normal	-134.974	32.020	-4.215	< .001
	V,Normal	-91.135	42.055	-2.167	0.375
N,Normal	S,Normal	-41.152	27.995	-1.470	0.823
	V,Normal	2.688	39.077	0.069	1.000
S,Normal	V,Normal	43.840	38.557	1.137	0.948

Supplementary Table S4, related to Fig. 7

Gene name	Parameter	non-SZ	SZ (top4)	SZ (all)
		(default value)		
arrestin3b	Total molecules	7.05 x 10 ⁶	7.05 x 10 ⁶	7.26 x 10 ⁶
				(x 1.03)
transducin	Total molecules	1 x 10 ⁷	5.5 x 10 ⁶	5.5 x 10 ⁶
			(x 0.55)	(x 0.55)
recoverin2	Total molecules	1 x 10 ⁷	6.17 x 10 ⁶	6.17 x 10 ⁶
			(x 0.617)	(x 0.617)
GC3/GCAP	alpha max (µM/s)	60	165	185
			(x 2.75)	(x 2.75 x 1.12)
			GC3	GC3 + GCAP3
pde6c	total molecules	2 x 10 ⁶	2 x 10 ⁶	2.82 x 10 ⁶
				(x 1.41)
CNGs	Total molecules	1 x 10 ⁶	5.9 x 10⁵	5.9 x 10⁵
			(x 0.59)	(x 0.59)
grk1/7	Total molecules	2 x 10⁵	2 x 10⁵	1.98 x 10⁵
				(x 1.98)
rgs9	Total molecules	1 x 10⁵	1 x 10 ⁵	1.23 x 10⁵
				(x 1.23)
slc24a	Ca2+ extrusion rate (/s)	981.3558	981.3558	1079.49138
	v = 7			(x 1.1)